European Journal of Medicinal Chemistry 93 (2015) 1–8

Contents lists available at ScienceDirect

European Journal of Medicinal Chemistry

journal homepage: http://www.elsevier.com/locate/ejmech

Original article

# Synthesis and anticancer activities of ceritinib analogs modified in the terminal piperidine ring

Peng Wang [a, c], Jin Cai [b], Junqing Chen [b], Min Ji [c, *]

[a] Department of Biomedical Engineering, School of Engineering, China Pharmaceutical University, Nanjing 210009, China
[b] School of Chemistry & Chemical Engineering, Southeast University, Nanjing 210096, China
[c] School of Biological Science & Medical Engineering, Southeast University, Nanjing 210096, China

ARTICLE INFO

*Article history:*
Received 12 September 2014
Received in revised form
26 January 2015
Accepted 27 January 2015
Available online 28 January 2015

*Keywords:*
ALK
Ceritinib analogs
Anticancer
Synthesis

ABSTRACT

A series of new ceritinib analogs by extensive functionalization of the tail piperidine ring with various phosphamides and carbamates have been synthesized. All the ceritinib derivatives were evaluated for their cytotoxic activities against H2228 cell line. From the activity profile obtained, three of the tested compounds (compounds **4**, **7** and **9**) showed significant cytotoxic effects. Among these derivatives compound **9** was found to possess cytotoxicity that is better than standard drug ceritinib ($IC_{50} = 24$ nM). Moreover, compound **9** demonstrated robust tumor growth inhibition in vivo model.



## 1. Introduction

Cancer is a leading cause of death worldwide and the deaths are projected to continue rising with an estimated 13 million deaths in 2030 [1]. Although chemotherapy has been widely used to cancer therapy, there is an urgent need to find new drugs for this hard-to-treat disease. Since the first tyrosine kinase inhibitor for the treatment of a human cancer (imatinib/Gleevec for chronic myeloid leukemia) was approved by FDA in 2001, tyrosine kinase inhibitors (TKI) have become the mainstream of target chemotherapy [2,3]. The recent understanding of the molecular pathophysiology of tumor has highlighted that many tyrosine kinases are found upstream or downstream of epidemiologically relevant oncogenes or tumor suppressor, especially the receptor tyrosine kinases.

Anaplastic lymphoma kinase (ALK) was first identified in 1994 as a part of nucleophosmin NPM-ALK fusion gene in 60% of anaplastic large-cell lymphoma (ALCL), and in late 2007 EML4-ALK fusion gene was found in 3–7 % of non-small cell lung cancer [4,5]. ALK is a receptor tyrosine kinase, grouped together with leukocyte tyrosine kinase (LTK) to a subfamily within the insulin receptor (IR) superfamily. Up to present, ALK as a cancer therapy target makes it an attractive target for cancer therapeutic intervention. A variety of ALK inhibitors have been developed and examined in clinical trials, such as crizoitnib, ceritinib, alectinib (Fig. 1). Among them, crizotinib (Xalkori) was the first small molecule inhibitor which was approved as a treatment of NSCLC including ALK fusion gene, EML4-ALK by FDA in 2011 [6,7]. Although crizotinib was very effective for the treatment of ALK-positive NSCLC, acquired drug resistance caused by point-mutations of ALK has been identified in patients treated with crizotinib [8,9]. To overcome ALK mutations, the activity of second-generation ALK inhibitors in patients with crizotinib-resistant ALK-positive NSCLC is currently being assessed in ongoing studies. For example, ceritinib and alectinib have received Breakthrough Therapy designation by the U.S. Food and Drug Administration (FDA) for the treatment of patients with ALK-positive metastatic non-small cell lung cancer (NSCLC) who had progressed during treatment with, or were intolerant to, crizotinib [10,11]. A number of other potent and more specific ALK inhibitors, including X-396, ASP3026, AP26113 and TSR-011 are currently in phase 1/2 clinical trials. Recently, ceritinib has been granted accelerated approval by the FDA, offering a much-needed treatment option for patients with certain lung cancers who relapse after first-line therapy [12].

From the SAR and molecular model analysis of ceritinib, the central pyrimidine ring of ceritinib was critical for activity, which can make hydrogen bonds at the hinge area via the pyrimidine and

* Corresponding author.
*E-mail addresses:* wangpeng159seu@hotmail.com (P. Wang), jimin@seu.edu.cn (M. Ji).

http://dx.doi.org/10.1016/j.ejmech.2015.01.056
0223-5234/

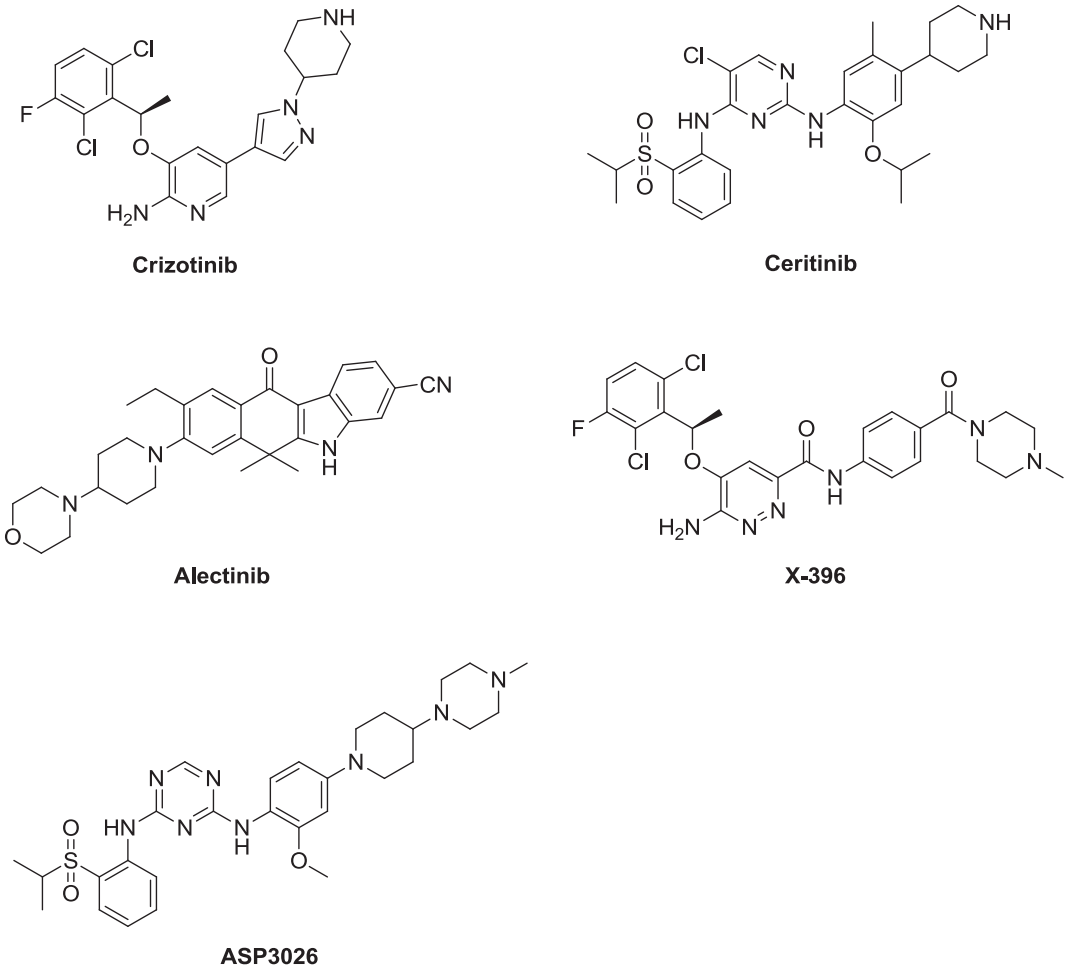


**Fig. 1.** Structures of selected ALK inhibitors.

amino nitrogen atoms. Although the substitutions on the nitrogen of the piperidine were fairly well-tolerated, the properties of substituents have significant influence on the ALK inhibition activity [13]. Moreover, the investigation of substituent groups on the nitrogen of the piperidine ring was not enough. In order to further study and improve the ALK inhibition activity, varieties of ceritinib derivatives were prepared and are reported herein, in which the nitrogen of piperidine has been replaced with various phosphamides and carbamates. The synthetic compounds were evaluated for their activity in vitro against H2228 NSCLC cell using MTS (3-(4,5-dimethylthiazol-2-yl)-5-(3-carboxymethoxyphenyl)-2-(4-sulfophenyl)-2*H*-tetrazolium) assay. The structure activity relationship (SAR) and biological properties of these newly synthesized molecules were compared to estimate its drug-likeliness and undesired properties.

## 2. Results and discussion

### 2.1. Chemistry

The syntheses for various ceritinib analogs require the corresponding ceritinib as the key intermediate (Scheme 1). Ceritinib can be successfully achieved in two steps starting with a modified Buchwald coupling reaction between 2,5-dichloro-*N*-(2-(isopropylsulfonyl)phenyl)pyrimidin-4-amine (**1**) and *tert*-butyl 4-(4-amino-5-isopropoxy-2-methylphenyl)piperidine-1-carboxylate (**2**) to form the C–N bond in good yield. Then deprotection of Boc group in the presence of TFA produced to the desired ceritinib in satisfactory yield. 2,5-Dichloro-*N*-(2-(isopropylsulfonyl)phenyl) pyrimidin-4-amine (**1**) was prepared from 1-fluoro-2-nitrobenzene via nucleophilic substitution with isopropyl mercaptan, oxidation of sulfide, reduction of nitro group, and nucleophilic substitution with 2,4,5-trichloropyrimidine. *tert*-Butyl 4-(4-amino-5-isopropoxy-2-methylphenyl)piperidine-1-carboxylate (**2**) can be obtained starting with 2- chloro-4-fluoro-1-methylbenzene in five steps as previously described [14].

Compounds **3a**–**c** were prepared in one step process in which ceritinib was respectively reacted with diethyl chlorophosphate, diphenyl chlorophosphate and dibenzyl chlorophosphate in excellent yields. Dibenzyl chlorophosphate was achieved by the chlorination of dibenzyl phosphite with *N*-chlorosuccinimide (NCS). The deprotection of benzyl group of compound **3c** can proceed smoothly to afford **4** in presence of TEA. The carbamate derivatives **5a**–**d** were obtained in good yields by the reaction of ceritinib with corresponding chloroformates in presence of DMAP and DCM.

With a view to increase the diversity of the library, functionalization of carbamate derivatives was taken up. Ceritinib was firstly reacted with chloromethyl chloroformate to give intermediate **6**, which was followed by reacting with potassium acetate to afford target compound **7**. Similarly, the products **8** and **9** were obtained in excellent yields. The new compounds thus synthesized are completely characterized by their spectral data before proceeding for biological evaluation.

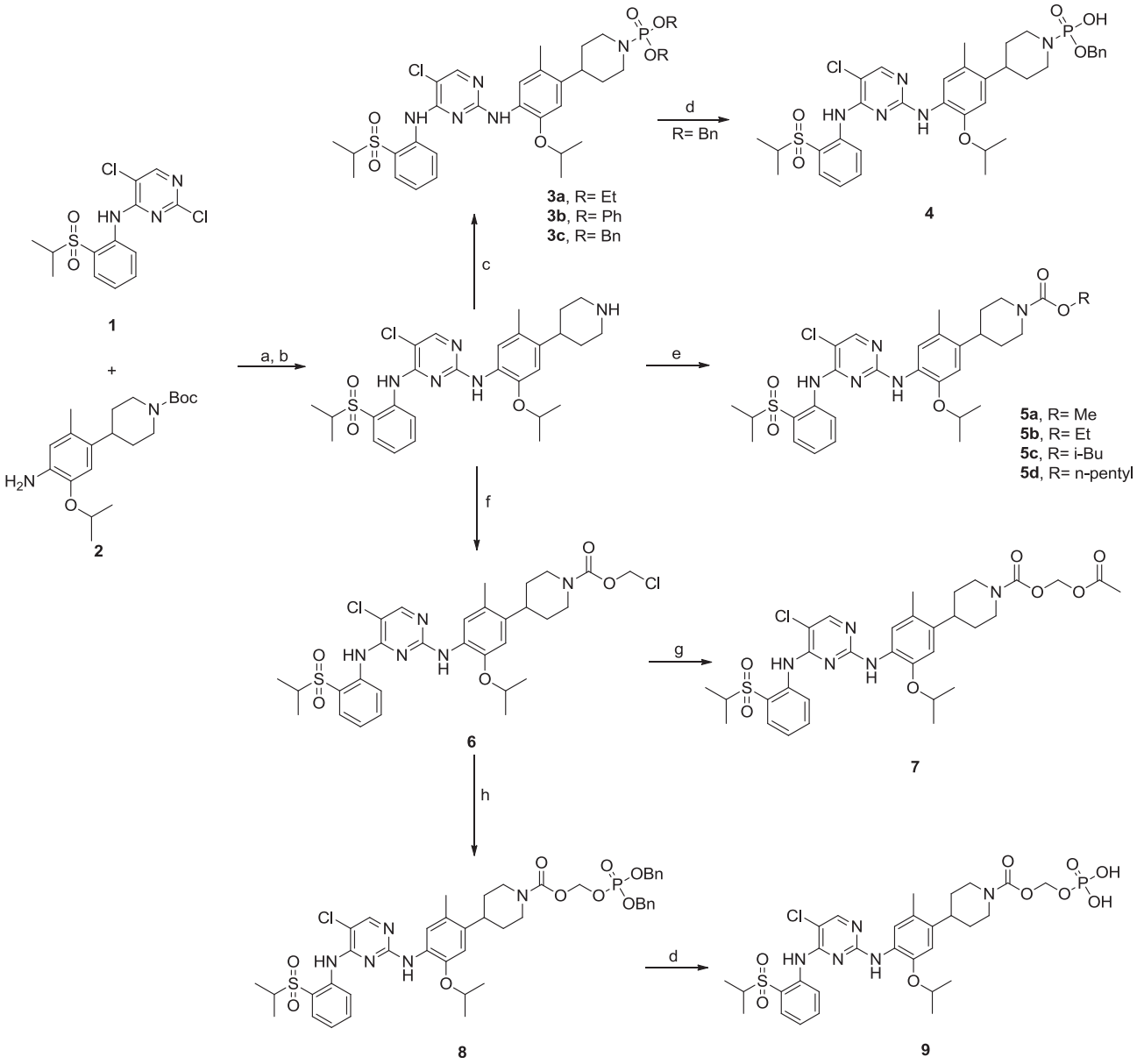


**Scheme 1.** The synthetic route of ceritinib analogs. Reagents and conditions: (a) $Pd(OAc)_2$, X-Phos, $Cs_2CO_3$, THF; (b) TFA, DCM, 50% yield over two steps; (c) $ClPO(OR)_2$, TEA, THF, 90%–96%; (d) $H_2$, Pd/C, TEA, THF, 97%–98%; (e) chloroformate, DMAP, DCM, 94%–96%; (f) chloromethyl chloroformate, DMAP, DCM, 63%; (g) $CH_3COOK$, DMF, 90%; (h) Dibenzyl phosphate silver salt, toluene, 80%.

### 2.2. Biological evaluations in vitro

All the synthesized compounds were evaluated for their in-vitro anticancer activity against the NSCLC human cell line H2228 and using ceritinib as a positive control. As shown in Table 1, three compounds (**4**, **7**, **9**) of the nine new compounds showed anti-H2228 $IC_{50}$ values between 24 and 120 nM. Compound **4** showed good anticancer activity with $IC_{50}$ values of 57 nM, which is about 2-fold more potent than that of ceritinib ($IC_{50}$ = 103 nM). The other ceritinib derivatives, compounds **3a**–**c** and **5a**–**d** exhibited a significant loss in potency compared to that of ceritinib. Moreover, the anticancer activity decreased obviously with the increase of alkyl chain. For example, compound **5a** (methyl) showed higher activity than compounds **5c** and **5d** (isobutyl and *n*-pentyl, respectively). It may be due to electromeric effect contributed by the alkyl groups being situated at the tail of ceritinib. Interestingly, compound **7** showed good anticancer activity with $IC_{50}$ values of 120 nM, which approached that of ceritinib. The most active compound of this set compound **9** gave a quite low $IC_{50}$ value of 24 nM, which is approximately 5-fold more potent than that of ceritinib. Compounds **8** (with $IC_{50}$ = 1037 nM), which is benzyl ester of **9**, exhibited a significant loss in potency compared to that of compound **9**. Compounds **4** and **9** are the most potent ones in *vitro* test.

### 2.3. Structure–activity relationship using docking studies

To predict the binding mode of the newly synthesized compounds, a docking study of compound **9** was first performed using AutoDock Vina. The X-ray crystal structure of ceritinib with the kinase domain of ALK taken from PDB (4MKC) was used as the input structure. Our findings suggested that compound **9** exhibited a similar binding mode with ceritinib. Compound **9** makes hydrogen

**Table 1**
Activity profile of ceritinib analogs on H2228 cell.

| Entry | Compound name | $IC_{50}$ (nM) |
|---|---|---|
| 3a | 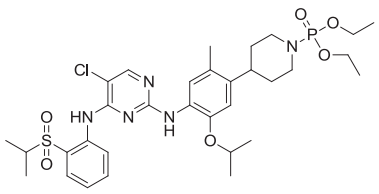 | 570.70 |
| 3b | 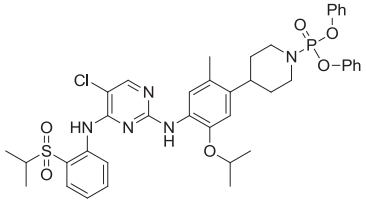 | 14355.00 |
| 3c | 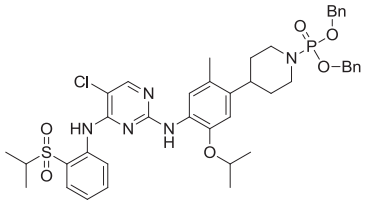 | 2691.00 |
| 4 | 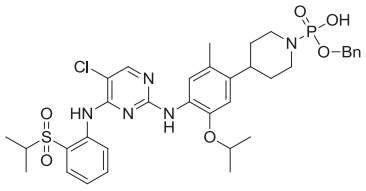 | 57.38 |
| 5a | 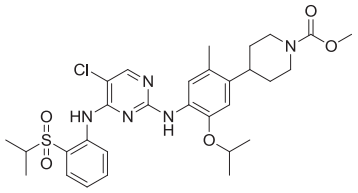 | 1114.00 |
| 5b | 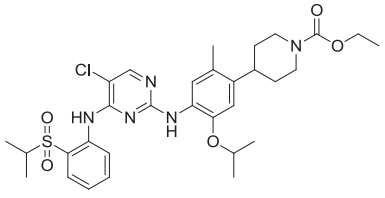 | 1195.00 |
| 5c | 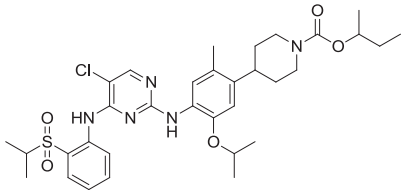 | 7404.00 |
| 5d | 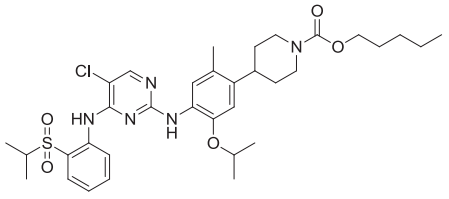 | 67157.00 |

**Table 1** (*continued*)

| Entry | Compound name | $IC_{50}$ (nM) |
|---|---|---|
| 7 | 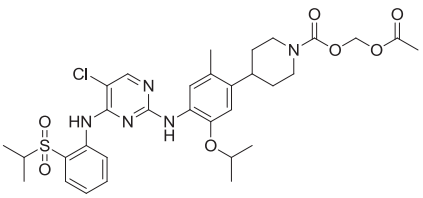 | 119.90 |
| 8 | 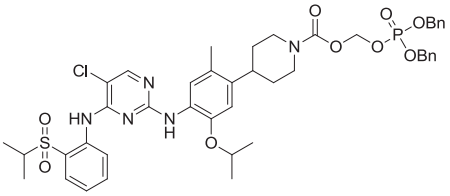 | 1037.00 |
| 9 | 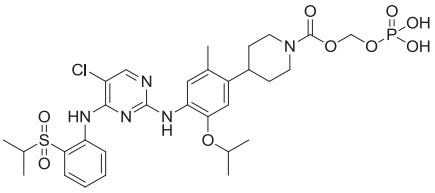 | 23.97 |
| Ceritinib | 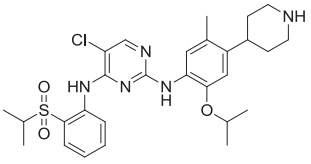 | 102.60 |

bonds at the hinge area via the pyrimidine and amino nitrogen atoms onto the backbone nitrogen and oxygen of Met1199 respectively. The tail of **9** which has phosphate group is pushed up into the solvent. Importantly, the carbonyl oxygen atom of carbamate group makes a hydrogen bond with Ser1206 and its carboxyl hydrogen atoms make hydrogen bonds with Glu1210 and Gly1201 respectively (Fig. 2). The fact that **9** has increased surface contact with protein leads to its better activity. Taken together, our molecular simulation allowed us to rationalize the activity profile of the ceritinib derivatives against ALK, which provided valuable information for further design of novel effective ALK inhibitors.

### 2.4. Biological evaluations in vivo

Although compound **4** showed potent anticancer activity, it was not evaluated in *vivo* because of its poor physicochemical property. To evaluate the antitumor efficacy of compounds **7** and **9**, a mouse tumor xenograft study was performed. Dosing started from day 15 post-cell implantation with tumor size around 150 $mm^3$. As illustrated in Fig. 3, untreated mice (vehicle) exhibited a rapid tumor growth, with tumor volumes of approximately 420 $mm^3$ at day 15. Compound **7** gave weak antitumor activity and hardly controlled tumor growth in *vivo*. Mice treated with compound **7** were slightly better than control group. In contrast, treatment of mice with compound **9** at the equivalent mole dose led to a considerable decrease in the tumor progression. Compound **9** showed significant tumor growth regression on day 15, with tumor growth inhibition as high as 80%. Moreover, its antitumor efficacy approached that of ceritinib at the end of the treatment. Similarly to observed in the cell culture experiments, compound **9** demonstrated greater in *vivo* anticancer activity than compound **7**. The relative body-weight loss

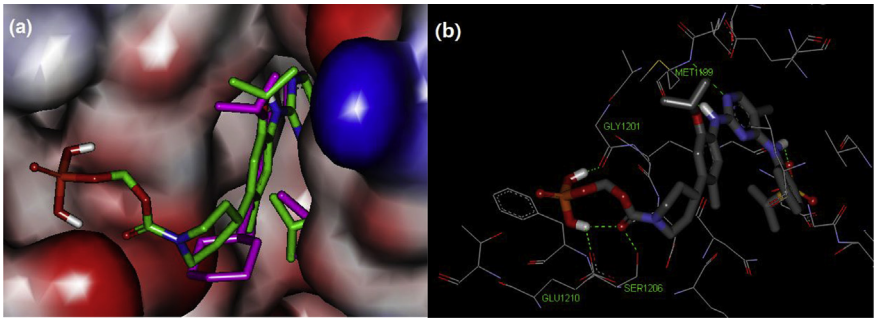


**Fig. 2.** (a) The binding models of ceritinib (pink) and 9 (green) with ALK; (b) Hydrogen bonding interactions between compound **9** and key amino acid residues. (For interpretation of the references to colour in this figure legend, the reader is referred to the web version of this article.)

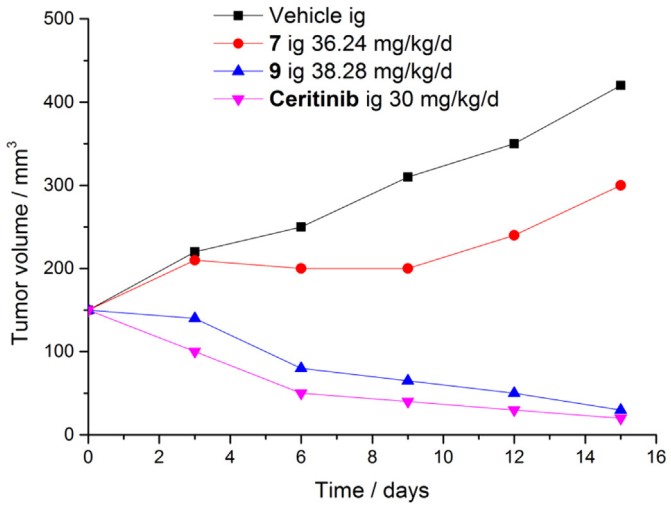


**Fig. 3.** Efficacy of **7** and **9** in 15-day rat xenograft H2228 model.

was also monitored throughout the treatment (Fig. 4). The results showed that no significant body weight reduction was observed throughout the course of the study, indicating there are no obvious adverse effects.

Because the chemical structure of compounds **7** and **9** are similar to prodrugs. We considered whether these compounds perform as prodrug in *vivo*. Then the pharmacokinetic profile of compounds **7** and **9** was compared to that of ceritinib according to plasma concentration after oral administration of compounds **7**, **9** and ceritinib. The plasma concentration profile versus time is shown in Fig. 5. A single dose of ceritinib, orally administrated, was rapidly absorbed and can be highly detected within 24 h. In contrast, plasma concentrations of ceritinib released from compounds **7** and **9** were significantly lower than those of ceritinib within 24 h. Therefore, prodrug principle was not the main mechanisms of the antitumor effect of the two compounds.

## 3. Conclusion

In summary, present work describes the synthesis of a series of ceritinib analogs by extensive functionalization of the tail piperidine ring with various phosphamides and carbamates. All the compounds synthesized were tested for anticancer activity against H2228 cell line. Three of the tested compounds (compounds **4**, **7** and **9**) showed significant cytotoxic effects with $IC_{50}$ values < 120 nM. Among these derivatives compound **9** exhibited better inhibitory activity than the standard ceritinib against H2228 cell line ($IC_{50}$ = 24 nM). Moreover, compound **9** demonstrated robust tumor growth inhibition in vivo model. We are currently engaged in a more detailed mechanistic investigation of **9** and will report our findings in due course.

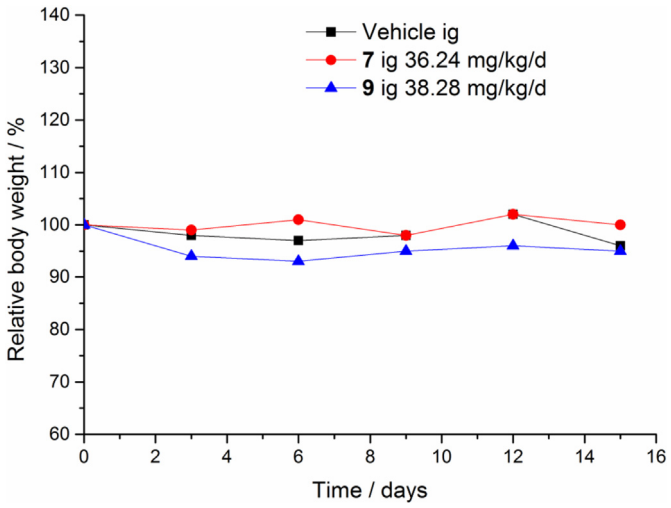


**Fig. 4.** Relative body weight as a function of time.

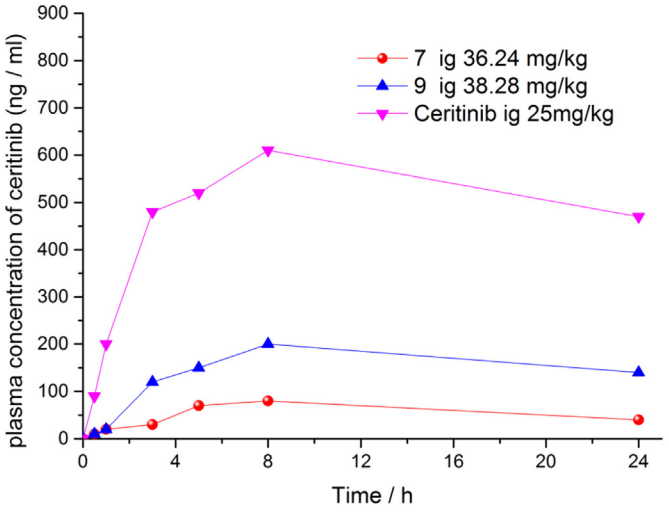


**Fig. 5.** Plasma concentration time profile of ceritinib upon oral administration of ceritinib itself and of compounds **7** and **9**.

## 4. Experimental section

### 4.1. Materials and methods

Commercial reagents were used as received. Analytical-grade solvents and commercially available reagents were used without further purification. Analytical thin layer chromatography (TLC) was performed on precoated silica gel $GF_{254}$ plates. Yields refer to the isolated yields of the products after purification by silica-gel column chromatography (200–300 mesh). Nuclear magnetic resonance (NMR) spectra were recorded on a Bruker-300 MHz spectrometer. Chemical shifts are reported relative to TMS; coupling constants are given in hertz. Mass data (ESI) were recorded by quadruple mass spectrometry.

### 4.2. General method for the preparation of compounds **3a**–**c**

To a mixture of ceritinib (200 mg, 0.358 mmol) and TEA (51 mg, 0.502 mmol) in dry THF (10 mL), diethyl chlorophosphate or diphenyl chlorophosphate or dibenzyl chlorophosphate (each 0.43 mmol) was added by a syringe. The reaction mixture was stirred at room temperature for about 24 h until the starting material disappeared by TLC. After the reaction was completed, the reaction mixture was concentrated to afford the crude product, which was purified by silica gel column chromatography to give compound **3a**–**c** respectively.

#### 4.2.1. Diethyl (4-(4-((5-chloro-4-((2-(isopropylsulfonyl)phenyl) amino)pyrimidin-2-yl)amino)-5-isopropoxy-2-methylphenyl) piperidin-1-yl)phosphonate (**3a**)

Yield: 90%; $^1$H NMR ($CDCl_3$) $\delta$: 1.33–1.43 (m, 18H), 1.55–1.76 (m, 4H), 2.16 (s, 3H), 2.75–2.90 (m, 3H), 3.21–3.30 (m, 1H), 3.70 (m, 2H), 4.03–4.13 (m, 4H), 4.49–4.57 (m, 1H), 6.73 (s, 1H), 7.26 (m, 2H), 7.60 (t, $J$ = 7.2 Hz, 1H), 7.92 (d, $J$ = 8.0 Hz, 1H), 7.95 (s, 1H), 8.13 (s, 1H), 8.56 (d, $J$ = 8.4 Hz, 1H), 9.60 (s, 1H); $^{13}$C NMR ($CDCl_3$) $\delta$: 15.3, 16.2, 16.3, 18.9, 22.2, 32.8, 32.9, 38.2, 45.5, 55.5, 71.7, 105.7, 111.1, 121.2, 123.3, 123.7, 125.1, 126.9, 131.3, 134.6, 138.2, 145.1, 155.5; $^{31}$P NMR ($CDCl_3$) $\delta$: 9.02; MS $m/z$: 694.3 $[M+H]^+$, 716.3 $[M+Na]^+$.

#### 4.2.2. Diphenyl (4-(4-((5-chloro-4-((2-(isopropylsulfonyl)phenyl) amino)pyrimidin-2-yl)amino)-5-isopropoxy-2-methylphenyl) piperidin-1-yl)phosphonate (**3b**)

Yield: 95%; $^1$H NMR (DMSO-*d*6) $\delta$: 1.15 (d, $J$ = 6.8 Hz, 6H), 1.21 (d, $J$ = 6.0 Hz, 6H), 1.55–1.59 (m, 2H), 2.08 (s, 3H), 2.71–2.95 (m, 3H), 3.39–3.45 (m, 1H), 3.48–3.73 (m, 4H), 4.34–4.43 (m, 1H), 6.37 (s, 1H), 7.21 (m, 2H), 7.33 (m, 5H), 7.45–7.48 (m, 5H), 7.57 (t, $J$ = 7.9 Hz, 1H), 7.84 (d, $J$ = 7.8 Hz, 1H), 8.08 (s, 1H), 8.24 (s, 1H), 8.42 (d, $J$ = 8.4 Hz, 1H), 9.48 (s, 1H); $^{13}$C NMR (DMSO-*d*6) $\delta$: 14.7, 18.2, 21.7, 31.8, 36.7, 44.9, 54.7, 70.7, 104.2, 111.2, 119.8, 119.9, 120.0, 123.5, 123.6, 123.9, 124.5, 124.8, 126.3, 126.7, 129.3, 129.8, 130.8, 134.6, 137.9, 138.8, 146.5, 150.3, 150.4, 154.8, 155.1, 157.8; $^{31}$P NMR (DMSO-*d*6) $\delta$: −0.68; MS $m/z$: 790.5 $[M+H]^+$, 812.5 $[M+Na]^+$.

#### 4.2.3. Dibenzyl (4-(4-((5-chloro-4-((2-(isopropylsulfonyl)phenyl) amino)pyrimidin-2-yl)amino)-5-isopropoxy-2-methylphenyl) piperidin-1-yl)phosphonate (**3c**)

Yield: 96%; $^1$H NMR (DMSO-*d*6) $\delta$: 1.14–1.20 (m, 12H), 1.59–1.62 (m, 2H), 2.11 (s, 3H), 2.57 (m, 1H), 2.75–2.86 (m, 3H), 3.38–3.56 (m, 4H), 4.42–4.49 (m, 1H), 5.02 (d, $J$ = 7.8 Hz, 4H), 6.69 (s, 1H), 7.32–7.44 (m, 11H), 7.52 (s, 1H), 7.60 (t, $J$ = 7.9 Hz, 1H), 7.84 (d, $J$ = 7.8 Hz, 1H), 8.05 (s, 1H), 8.25 (s, 1H), 8.45 (d, $J$ = 8.4 Hz, 1H), 9.47 (s, 1H); $^{13}$C NMR (DMSO-*d*6) $\delta$: 14.7, 18.2, 21.7, 29.4, 32.1, 32.2, 37.3, 44.8, 54.8, 66.9, 67.0, 70.7, 104.2, 111.7, 123.5, 123.6, 123.7, 124.4, 126.4, 126.8, 127.5, 127.9, 128.3, 130.8, 134.7, 136.7, 136.8, 137.9, 139.0, 146.4, 154.8, 155.1, 157.8; $^{31}$P NMR (DMSO-*d*6) $\delta$: 9.45; MS $m/z$: 818.5 $[M+H]^+$, 840.5 $[M+Na]^+$.

### 4.3. Procedures for the synthesis of benzyl hydrogen (4-(4-((5-chloro-4-((2-(isopropylsulfonyl)phenyl)amino)pyrimidin-2-yl) amino)-5-isopropoxy-2-methylphenyl)piperidin-1-yl)phosphonate (**4**)

Compound **3c** (300 mg, 0.367 mmol) was dissolved in dry THF (10 mL). Then TEA (0.3 mL) and 10% Pd/C (30 mg) was added to the mixture. The mixture was stirred at room temperature under hydrogen for overnight. The reaction mixture was filtered and concentrated under vacuum to afford compound **4**. Yield: 97%; $^1$H NMR (DMSO-*d*6) $\delta$: 1.14–1.21 (m, 12H), 1.58–1.64 (m, 2H), 2.11 (s, 3H), 2.59 (m, 1H), 2.75–2.87 (m, 3H), 3.36–3.57 (m, 4H), 4.42–4.48 (m, 1H), 5.05 (d, $J$ = 7.8 Hz, 2H), 6.71 (s, 1H), 7.33–7.46 (m, 6H), 7.55 (s, 1H), 7.60 (t, $J$ = 7.9 Hz, 1H), 7.84 (d, $J$ = 7.8 Hz, 1H), 8.04 (s, 1H), 8.25 (s, 1H), 8.46 (d, $J$ = 8.4 Hz, 1H), 9.48 (s, 1H). $^{13}$C NMR (DMSO-*d*6) $\delta$: 14.7, 18.3, 21.7, 29.5, 32.0, 32.2, 37.6, 44.8, 54.9, 66.9, 67.0, 70.9, 104.2, 111.8, 123.5, 123.6, 123.7, 124.5, 126.4, 126.9, 127.5, 127.9, 128.6, 130.8, 134.7, 136.7, 136.8, 137.8, 139.1, 146.4, 154.9, 155.2, 157.8. $^{31}$P NMR (DMSO-*d*6) $\delta$: 5.98. MS $m/z$: 728.4 $[M+H]^+$.

### 4.4. General method for the preparation of compounds **5a**–**d**

Chloroformate (0.4 mmol) was added to the mixture of ceritinib (150 mg, 0.27 mmol) and DMAP (99 mg, 0.81 mmol) in dry dichloromethane (10 mL). The reaction mixture was stirred at room temperature for overnight. Dichloromethane was removed under reduced pressure and purified by column chromatography to afford the desired product.

#### 4.4.1. Methyl 4-(4-((5-chloro-4-((2-(isopropylsulfonyl)phenyl) amino)pyrimidin-2-yl)amino)-5-isopropoxy-2-methylphenyl) piperidine-1-carboxylate (**5a**)

Yield: 95%; $^1$H NMR ($CDCl_3$) $\delta$: 1.23–1.37 (m, 12H), 1.55–1.78 (m, 4H), 2.17 (s, 3H), 2.79–2.92 (m, 3H), 3.21–3.30 (m, 1H), 3.73 (s, 3H), 4.30 (m, 2H), 4.50–4.58 (m, 1H), 6.70 (s, 1H), 7.26 (m, 1H), 7.57–7.64 (m, 2H), 7.93 (d, $J$ = 8.0 Hz, 1H), 8.01 (s, 1H), 8.15 (s, 1H), 8.57 (d, $J$ = 8.4 Hz, 1H), 9.52 (s, 1H); $^{13}$C NMR ($CDCl_3$) $\delta$: 15.3, 18.9, 22.2, 32.5, 38.1, 44.7, 52.5, 55.4, 71.6, 105.8, 110.8, 120.7, 123.1, 123.6, 124.9, 126.8, 127.7, 131.2, 134.5, 137.0, 138.4, 144.7, 155.1, 155.3, 155.9, 157.4; MS $m/z$: 638.3 $[M+Na]^+$.

#### 4.4.2. Ethyl 4-(4-((5-chloro-4-((2-(isopropylsulfonyl)phenyl) amino)pyrimidin-2-yl)amino)-5-isopropoxy-2-methylphenyl) piperidine-1-carboxylate (**5b**)

Yield: 94%; $^1$H NMR (DMSO-*d*6) $\delta$: 1.04–1.21 (m, 15H), 1.53–1.65 (m, 4H), 2.14 (s, 3H), 2.83–2.87 (m, 3H), 3.43 (m, 1H), 4.04–4.16 (m, 4H), 4.58–4.61 (m, 1H), 6.84 (s, 1H), 7.33–7.38 (m, 1H), 7.54 (s, 1H), 7.60–7.63 (m, 1H), 7.84 (d, $J$ = 7.8 Hz, 1H), 8.01 (s, 1H), 8.24 (s, 1H), 8.47 (d, $J$ = 8.1 Hz, 1H), 9.46 (s, 1H); $^{13}$C NMR (DMSO-*d*6) $\delta$: 14.5, 14.7, 18.3, 21.8, 31.9, 37.4, 44.0, 54.7, 60.5, 70.6, 104.2, 111.7, 123.5, 123.6, 124.4, 126.3, 126.7, 130.8, 134.7, 137.9, 138.8, 146.4, 154.4, 154.8, 155.3, 157.9; MS $m/z$: 630.4 $[M+H]^+$, 652.4 $[M+Na]^+$.

#### 4.4.3. sec-Butyl 4-(4-((5-chloro-4-((2-(isopropylsulfonyl)phenyl) amino)pyrimidin-2-yl)amino)-5-isopropoxy-2-methylphenyl) piperidine-1-carboxylate (**5c**)

Yield: 95%; $^1$H NMR ($CDCl_3$) $\delta$: 0.95 (d, $J$ = 6.6 Hz, 6H), 1.31 (d, $J$ = 6.0 Hz, 6H), 1.36 (d, $J$ = 6.0 Hz, 6H), 1.56–1.60 (m, 2H), 1.74–1.79 (m, 2H), 1.91–2.03 (m, 1H), 2.15 (s, 3H), 2.79–2.92 (m, 3H), 3.21–3.30 (m, 1H), 3.90 (d, $J$ = 6.4 Hz, 2H), 4.30–4.34 (m, 2H), 4.49–4.57 (m, 1H), 6.71 (s, 1H), 7.23–7.28 (m, 1H), 7.59–7.64 (m, 2H), 7.93 (d, $J$ = 7.9 Hz, 1H), 8.00 (s, 1H), 8.15 (s, 1H), 8.57 (d, $J$ = 8.4 Hz, 1H), 9.52 (s, 1H); $^{13}$C NMR ($CDCl_3$) $\delta$: 15.3, 18.9, 19.1, 22.2,

28.0, 32.6, 38.2, 44.7, 55.4, 71.5, 71.6, 105.8, 110.9, 120.8, 123.1, 123.6, 124.9, 126.8, 127.7, 131.2, 134.6, 137.1, 138.4, 144.8, 155.1, 155.4, 155.6, 157.4; MS *m/z*: 680.4 $[M+Na]^+$.

#### 4.4.4. Pentyl 4-(4-((5-chloro-4-((2-(isopropylsulfonyl)phenyl)amino)pyrimidin-2-yl)amino)-5-isopropoxy-2-methylphenyl)piperidine-1-carboxylate (**5d**)

Yield: 96%; $^1$H NMR ($CDCl_3$) $\delta$: 0.92 (m, 3H), 1.31–1.38 (m, 16H), 1.56–1.78 (m, 6H), 2.17 (s, 3H), 2.83–2.91 (m, 3H), 3.21–3.31 (m, 1H), 4.11 (t, $J$ = 9.6 Hz, 2H), 4.30 (m, 2H), 4.50–4.58 (m, 1H), 6.71 (s, 1H), 7.24–7.29 (m, 1H), 7.59–7.64 (m, 2H), 7.93 (d, $J$ = 7.7 Hz, 1H), 8.00 (s, 1H), 8.15 (s, 1H), 8.57 (d, $J$ = 8.4 Hz, 1H), 9.53 (s, 1H); $^{13}$C NMR ($CDCl_3$) $\delta$: 13.9, 15.3, 18.9, 22.2, 22.3, 28.1, 28.7, 32.6, 38.2, 44.7, 55.5, 65.5, 71.6, 105.8, 110.9, 120.8, 123.1, 123.6, 125.0, 126.8, 127.6, 131.2, 134.6, 137.2, 138.4, 142.7, 144.8, 154.9, 155.4, 155.6, 157.3; MS *m/z*: 672.4 $[M+H]^+$, 694.4 $[M+Na]^+$.

### 4.5. Procedures for the synthesis of acetoxymethyl 4-(4-((5-chloro-4-((2-(isopropylsulfonyl)phenyl)amino)pyrimidin-2-yl)amino)-5-isopropoxy-2-methylphenyl)piperidine-1-carboxylate (**7**)

Chloromethyl chloroformate (194 mg, 2.0 mmol) was added to the mixture of ceritinib (558 mg, 1.0 mmol) and DMAP (305 mg, 2.5 mmol) in dry dichloromethane (10 mL) under 0 °C. The reaction mixture was stirred at room temperature for overnight. Dichloromethane was removed under reduced pressure and purified by column chromatography to afford compound **6** in 63% yield. Then compound **6** (200 mg, 0.3 mmol) and potassium acetate (98 mg, 1.0 mmol) was added to DMF (10 mL). The mixture was reacted at 80 °C for 4 h. The solvent was removed under reduced pressure and purified by column chromatography to afford compound **7**. Yield: 90%; $^1$H NMR ($CDCl_3$) $\delta$: 1.32 (d, J = 6.8 Hz, 6H), 1.36 (d, $J$ = 6 Hz, 6H), 1.59 (m, 2H), 1.77 (m, 2H), 2.13 (s, 3H), 2.17 (s, 3H), 2.80–2.93 (m, 3H), 3.21–3.30 (m, 1H), 4.30–4.35 (m, 2H), 4.50–4.58 (m, 1H), 5.80 (s, 2H), 6.69 (s, 1H), 7.24–7.29 (m, 1H), 7.59–7.64 (m, 2H), 7.93 (d, $J$ = 7.8 Hz, 1H), 8.00 (s, 1H), 8.15 (s, 1H), 8.57 (d, $J$ = 8.3 Hz, 1H), 9.55 (s, 1H); $^{13}$C NMR ($CDCl_3$) $\delta$: 15.3, 18.9, 20.9, 22.2, 32.2, 32.6, 38.0, 44.9, 55.5, 71.7, 80.4, 105.8, 110.9, 120.9, 123.2, 123.6, 125.0, 126.9, 127.7, 131.3, 134.6, 136.9, 138.4, 144.9, 153.5, 154.8, 155.4, 157.2, 169.9; MS *m/z*: 674.4 $[M+H]^+$, 696.3 $[M+Na]^+$.

### 4.6. Procedures for the synthesis of ((bis(benzyloxy)phosphoryl)oxy)methyl 4-(4-((5-chloro-4-((2-(isopropylsulfonyl)phenyl)amino)pyrimidin-2-yl)amino)-5-isopropoxy-2-methylphenyl)piperidine-1-carboxylate (**8**)

Compound **6** (400 mg, 0.6 mmol) and dibenzyl phosphate silver salt (710 mg, 1.84 mmol) was added to toluene (20 mL). The mixture was refluxed for 4 h. The solvent was removed under reduced pressure and purified by column chromatography using ethyl acetate as eluant to afford compound **8**. Yield: 80%; $^1$H NMR (DMSO-*d*6) $\delta$: 1.14–1.18 (m, 12H), 1.53–1.67 (m, 4H), 2.14 (s, 3H), 2.90 (m, 3H), 3.38–3.48 (m, 1H), 4.06–4.17 (m, 2H), 4.48–4.56 (m, 1H), 5.08 (d, $J$ = 7.8 Hz, 4H), 5.66 (d, $J$ = 13.3 Hz, 2H), 6.79 (s, 1H), 7.38 (m, 11H), 7.54 (s, 1H), 7.62 (t, $J$ = 7.9 Hz, 1H), 7.84 (d, $J$ = 7.8 Hz, 1H), 8.04 (s, 1H), 8.25 (s, 1H), 8.46 (d, $J$ = 8.3 Hz, 1H), 9.47 (s, 1H). $^{13}$C NMR (DMSO-*d*6) $\delta$: 14.7, 18.3, 21.7, 31.6, 31.8, 37.1, 44.2, 54.7, 68.6, 68.7, 70.6, 83.6, 83.7, 104.2, 111.6, 123.4, 123.5, 124.4, 126.3, 126.8, 127.7, 128.3, 128.4, 130.8, 134.7, 135.7, 137.9, 138.5, 146.4, 152.2, 154.7, 155.3, 157.8. $^{31}$P NMR (DMSO-*d*6) $\delta$: −2.24. MS *m/z*: 914.5 $[M+Na]^+$.

### 4.7. Procedures for the synthesis of (phosphonooxy)methyl 4-(4-((5-chloro-4-((2-(isopropylsulfonyl)phenyl)amino)pyrimidin-2-yl)amino)-5-isopropoxy-2-methylphenyl)piperidine-1-carboxylate (**9**)

Compound **8** (200 mg, 0.224 mmol) was dissolved in dry THF (10 mL). Then TEA (0.2 mL) and 10% Pd/C (20 mg) was added to the mixture. The mixture was stirred at room temperature under hydrogen for overnight. The reaction mixture was filtered and concentrated under vacuum to afford compound **9**. Yield: 98%; $^1$H NMR (DMSO-*d*6) $\delta$: 1.14–1.19 (m, 12H), 1.53–1.65 (m, 4H), 2.13 (s, 3H), 2.92 (m, 3H), 3.38–3.48 (m, 1H), 4.05–4.18 (m, 2H), 4.47–4.55 (m, 1H), 5.67 (d, $J$ = 13.3 Hz, 2H), 6.81 (s, 1H), 7.28 (m, 1H), 7.54 (s, 1H), 7.62 (t, $J$ = 7.9 Hz, 1H), 7.84 (d, $J$ = 7.8 Hz, 1H), 8.07 (s, 1H), 8.26 (s, 1H), 8.44 (d, $J$ = 8.3 Hz, 1H), 9.47 (s, 1H). $^{13}$C NMR (DMSO-*d*6) $\delta$: 15.3, 18.9, 21.7, 28.1, 29.4, 37.1, 44.2, 55.4, 70.6, 83.6, 83.7, 104.2, 111.8, 123.4, 123.5, 124.4, 126.3, 126.9, 130.7, 134.8, 135.6, 137.9, 138.4, 146.4, 152.3, 154.8, 155.5, 157.9. $^{31}$P NMR (DMSO-*d*6) $\delta$: −1.96. MS *m/z*: 712.3 $[M+H]^+$.

### 4.8. Biology

#### 4.8.1. In vitro antitumor activity assays

The cytotoxicity was measured by the MTS assay as described in the literature. Briefly, H2228 cells were seeded in 96-well plates. After 24 h of cultivation, the cells were treated in triplicate with various concentrations of compounds for 72 h in 5% $CO_2$ incubator at 37 °C. Cell viability was measured using MTS [3-(4,5-dimethylthiazol-2-yl)-5-(3-carboxymethoxyphenyl)-2-(4-sulfophenyl)-2H-tetrazolium] assay. In short, 20 μL of MTS (5 mg/mL) solution were added to each well. The plate was incubated for an additional 4 h, and then the medium was removed. The plates were vigorously shaken before taking measurement of relative color intensity. The absorbance of each well was measured by a microplate reader at a test wavelength of 570 nm. The cell inhibitory rate was calculated and the cytotoxicities of compounds were expressed as $IC_{50}$ that was defined as the drug concentration required inhibiting growth by 50% relative to controls.

#### 4.8.2. In vivo antitumor assays

RNU nude rats bearing the H2228 tumors were randomized into four groups (n = 6 rats per group) with an average tumor size of 150 $mm^3$. Compounds 7, 9 and ceritinib was formulated in 0.5% MC/0.5% Tween 80 and administered by oral gavage at a dosing volume of 10 μL/g of an animal body weight. Animals in each group received vehicle, compounds **7**, **9** or ceritinib every day for 14 consecutive days. During treatment, body weight was monitored regularly. Tumor volume was calculated by the formula ($V = ab^2/2$, where $a$ and $b$ stand for the longest and shortest diameter, respectively). After treated for 14 days with drugs, the animals were sacrificed and solid tumors were removed and weighted. The inhibition rate was calculated as [(averaged tumor weight of the control group − averaged tumor weight of drug-treated group)/averaged tumor weight of the control group] × 100%.

SD male rats (weight 200–220 g) were randomized into three groups (n = 4 rats per group). Compounds **7**, **9** and ceritinib was formulated in 0.5% MC/0.5% Tween 80 and administered by oral gavage at a dosing volume of 10 μL/g of an animal body weight. Animals in each group received compounds **7**, **9** or ceritinib. Plasma samples were collected 0.5, 1, 3, 5, 8 and 24 h after dosing. Aliquots of all biological matrixes were deproteinized with ethyl acetate. The suspension was vortexed, mixed, and centrifuged at 4000 rpm for 5 min. The organic phase was injected into the HPLC system.

### 4.9. Docking studies

Compound **9** was ultimately converted to the PDBQT format using AutoDock Tools [15], which is required for AutoDock Vina [16]. The 3-dimensional (3D) structure of ALK was downloaded from the Protein Data Bank (PDB ID: 4MKC). The molecular docking was conducted using AutoDock Vina, which uses a unique algorithm that implements a machine learning approach to its scoring function. Using AutoDock Tools, the PDB (4MKC) structure was converted from a pdb file to a pdbqt file. A grid box size of 20, 20, 20 Å was generated and allocated at the center of the receptor binding site using x, y and z coordinates of −21.253, 9.84 and −7.668. Then the compound **9** was docked into the binding site of ALK. For Vina docking, the default parameters were used if it was not mentioned. Docked structures were visualized using Discovery Studio Visualizer 2.5 (Accelrys Software Inc.).

## Acknowledgments

This study is supported by the Fundamental Research Funds for the Central Universities (ZJ15011), National Basic Research Program of China (No. 2011CB933503) and Technology Supporting Program of Jiangsu province (BE2009639, BE2012657).

## Appendix A. Supplementary data

Supplementary data related to this article can be found at http://dx.doi.org/10.1016/j.ejmech.2015.01.056.

## References

[1] P. Wang, J. Cai, J.Q. Chen, L.S. Li, C.L. Sun, B. Xue, M. Ji, 3D-QSAR and docking studies of piperidine carboxamide derivatives as ALK inhibitors, Med. Chem. Res. 23 (2014) 2576–2583.
[2] D.S. Krause, R.A. Van Etten, Tyrosine kinases as targets for cancer therapy, N. Engl. J. Med. 353 (2005) 172–187.
[3] A. Gschwind, O.M. Fischer, A. Ullrich, Timeline – the discovery of receptor tyrosine kinases: targets for cancer therapy, Nat. Rev. Cancer 4 (2004) 361–370.
[4] S.W. Morris, M.N. Kirstein, M.B. Valentine, K.G. Dittmer, D.N. Shapiro, D.L. Saltman, A.T. Look, Fusion of a kinase gene, Alk, to a Nucleolar protein gene, Npm, in non-Hodgkins-lymphoma, Science 263 (1994) 1281–1284.
[5] M. Soda, Y.L. Choi, M. Enomoto, S. Takada, Y. Yamashita, S. Ishikawa, S.I. Fujiwara, H. Watanabe, K. Kurashina, H. Hatanaka, M. Bando, S. Ohno, Y. Ishikawa, H. Aburatani, T. Niki, Y. Sohara, Y. Sugiyama, H. Mano, Identification of the transforming EML4-ALK fusion gene in non-small-cell lung cancer, Nature 448 (2007) 561–U563.
[6] J.E. Frampton, Crizotinib: a review of its use in the treatment of anaplastic lymphoma kinase-positive, advanced non-small cell lung cancer, Drugs 73 (2013) 2031–2051.
[7] A.T. Shaw, U. Yasothan, P. Kirkpatrick, Crizotinib, Nat. Rev. Drug Discov. 10 (2011) 897–898.
[8] S. Zhang, F. Wang, J. Keats, X.T. Zhu, Y.Y. Ning, S.D. Wardwell, L. Moran, Q.K. Mohemmad, R. Anjum, Y.H. Wang, N.I. Narasimhan, D. Dalgarno, W.C. Shakespeare, J.J. Miret, T. Clackson, V.M. Rivera, Crizotinib-resistant mutants of EML4-ALK identified through an accelerated mutagenesis Screen, Chem. Biol. Drug Des. 78 (2011) 999–1005.
[9] M. Ceccon, L. Mologni, W. Bisson, L. Scapozza, C. Gambacorti-Passerini, Crizotinib-resistant NPM-ALK mutants confer differential sensitivity to unrelated Alk inhibitors, Mol. Cancer Res. 11 (2013) 122–132.
[10] J.Y. Chen, C. Jiang, S.M. Wang, LDK378: a promising anaplastic lymphoma kinase (ALK) inhibitor, J. Med. Chem. 56 (2013) 5673–5674.
[11] S.H.I. Ou, M. Azada, D.J. Hsiang, J.M. Herman, T.S. Kain, C. Siwak-Tapp, C. Casey, J. He, S.M. Ali, S.J. Klempner, V.A. Miller, Next-generation sequencing reveals a novel NSCLC ALK F1174V mutation and confirms ALK G1202R mutation confers high-level resistance to alectinib (CH5424802/RO5424802) in ALK-rearranged NSCLC patients who progressed on Crizotinib, J. Thorac. Oncol. 9 (2014) 549–553.
[12] Ceritinib gains FDA approval for lung Cancer, Cancer Discov. 4 (2014) 753–754.
[13] T.H. Marsilje, W. Pei, B. Chen, W.S. Lu, T. Uno, Y.H. Jin, T. Jiang, S. Kim, N.X. Li, M. Warmuth, Y. Sarkisova, F. Sun, A. Steffy, A.C. Pferdekamper, A.G. Li, S.B. Joseph, Y. Kim, B. Liu, T. Tuntland, X.M. Cui, N.S. Gray, R. Steensma, Y.Q. Wan, J.Q. Jiang, G. Chopiuk, J. Li, W.P. Gordon, W. Richmond, K. Johnson, J. Chang, T. Groessl, Y.Q. He, A. Phimister, A. Aycinena, C.C. Lee, B. Bursulaya, D.S. Karanewsky, H.M. Seidel, J.L. Harris, P.Y. Michellys, Synthesis, structure-activity relationships, and in vivo efficacy of the novel potent and selective anaplastic lymphoma kinase (ALK) inhibitor 5-Chloro-N2-(2-isopropoxy-5-methyl-4-(piperidin-4-yl)phenyl)-N4-(2-(isopropylsulfonyl)phenyl)pyrimidine-2,4-diamine (LDK378) currently in phase 1 and phase 2 clinical trials, J. Med. Chem. 56 (2013) 5675–5690.
[14] B. Chen, T. Jiang, T.H. Marsilje, P.-Y. Michellys, T.N. Nguyen, W. Pei, B. Wu, Z. Gao, Y. Ge, C. Huang, Y. Li, Preparation of Pyrimidine Derivatives as Protein Kinase Inhibitors for Treating Proliferative Disorders, Immune Disorders, and Infections, IRM LLC, Bermuda, 2009, p. 149. Novartis A.-G.
[15] G.M. Morris, R. Huey, W. Lindstrom, M.F. Sanner, R.K. Belew, D.S. Goodsell, A.J. Olson, AutoDock4 and AutoDockTools4: automated docking with selective receptor flexibility, J. Comput Chem. 30 (2009) 2785–2791.
[16] O. Trott, A.J. Olson, AutoDock Vina: improving the speed and accuracy of docking with a new scoring function, efficient optimization, and multithreading, J. Comput Chem. 31 (2010) 455–461.